Astron. Astrophys. 213, 1–9 (1989)

ASTRONOMY AND ASTROPHYSICS

Fragmenting the universe

II. Voronoi vertices as Abell clusters

R. van de Weygaert and V. Icke

Sterrewacht Leiden, Postbus 9513, NL-2300 RA Leiden, The Netherlands

Received August 25, accepted September 16, 1988

Summary. The large-scale structure of the Universe (around 50 Mpc) can be described by means of "Voronoi foam", which is a partitioning of space obtained by a process called Voronoi tessellation. We present the first results of a comparison between the statistics of Voronoi foams and the observed galaxy distribution. In particular, we show that the spatial two-point correlation function of Voronoi vertices has a power law behaviour with almost the same amplitude and slope as that of the Abell clusters. This confirms our earlier expectations that Voronoi nodes are to be identified with high-density galaxy clusters in the Universe.

Key words: cosmology – clusters: of galaxies – correlation functions

1. The Voronoi model

In a pressureless, selfgravitating medium, fluctuations that have a density above average must collapse to form structures with increasingly aspherical shapes, becoming flattened and filamentary (Lynden-Bell, 1964; Lin et al., 1965; Icke, 1972). The secular increase of the asphericity of perturbations explains the filamentary appearance of the distribution of galaxies (Icke, 1973; Oort, 1983; Giovanelli et al., 1986; De Lapparent et al., 1986), but the approximation must break down as soon as the perturbations become nonlinear.

Contrariwise, low-density fluctuations expand a little faster than the average Hubble rate, becoming progressively more *spherical* as they expand (Icke, 1984). These fluctuations are the progenitors of the observed voids (Einasto et al., 1980; Kirshner et al., 1981, 1987). The same arguments as above can still be applied, except that the sense of the final effect is reversed: because a void is effectively a region of negative density in a uniform background, the voids expand while the overdense regions collapse, and slight asphericities decrease as the voids become larger. Consequently, the density in the voids becomes smaller in the course of time. Moreover, because $|\delta\varrho/\varrho|$ does not exceed unity in a void, the linear approximation will remain good for a longer period, except near the outer parts of the voids, where the matter gets swept up. Just as in the case of growing filaments, the velocity field in the voids is proportional to the distance inside them: voids are expected to be "superhubble bubbles."

Thus, we can "turn the Universe inside out", and consider the evolution of the *low*-density regions. We may then think of the large-scale structure [1] of gravitating matter in the Universe as a close packing of spheres, generating convex cells of different sizes out of which matter flows in a slightly super-Hubble expansion towards the interstices of the spheres.

In our description, the voids are driven by an effective expansion that is due to the presence of locally underdense regions. However, explicitly driven expansion, as in the case of explosion bubbles (Ikeuchi, 1981; Ostriker and Cowie, 1981), produces the same partitioning of space.

The above "Bubble Theorem" provides a physical mechanism behind the construction of the *skeleton* of the cosmic large-scale mass distribution by considering the locus of points towards which the matter streams out of the voids. Consider a collection of slightly underdense regions in the primordial density field. These regions are the seeds of voids, expansion centres from which matter flows away until it encounters similar material flowing out of an adjacent void. Making the approximation that the excess expansion is the same in all voids, the matter must collect on planes that perpendicularly bisect the axes connecting the expansion centres.

For any given set of expansion centres, or *nuclei*, the arrangement of these planes defines a unique process for the partitioning of space, a *Voronoi tessellation* (Voronoi, 1908). A particular realisation of this process may be called a *Voronoi foam* (Icke and Van de Weygaert, 1987). A Voronoi foam consists of a packing of Voronoi cells. Each cell that surrounds a particular nucleus encloses that part of space which is closer to its nucleus than to any other nucleus.

In three-space, such a foam is built of three topologically distinct elements: *walls*, formed by the planes that enclose the polyhedral Voronoi cells (the interiors of which are observed as voids), *filaments* where three walls intersect, and *nodes* where four filaments come together. The walls are "pancakes" (Zel'dovich, 1970), the filaments are supposed to correspond to the elongated superclusters (Icke, 1972; Oort, 1983; Giovanelli et al., 1986), and

Send offprint requests to: R. van de Weygaert

[1] This is the term commonly used for structures with length scales on the order of 100 Mpc. We prefer to call this a "medium" scale, in view of the fact that the horizon radius is two orders of magnitude larger. However, we will conform to present usage.

the nodes are identified with the Abell clusters (Icke and Van de Weygaert, 1987).

In principle, the Voronoi topology consists of a packing of closed, convex cells. However, one should distinguish between the mathematical Voronoi skeleton, and the actual mass density with which that skeleton is covered. As will be seen in the kinematic simulation to be presented below, the density in the centres of the walls decreases rapidly during the evolution of the cells; later, the density in the filaments decreases too, even as the matter streams towards the nodes. Thus, the walls become porous, leading to an actual matter distribution that is much more sponge-like (cf. Gott et al., 1986; Weinberg et al., 1987; Melott et al., 1988) than the pure Voronoi partitioning would suggest.

Icke and Van de Weygaert (1987) published an extensive analysis of planar Voronoi tessellations, for different arrangements of nuclei. The resulting Voronoi foams show a striking similarity with two-dimensional numerical simulations of gravitationally collapsing scale-free media (e.g. Melott, 1983; Matsuda and Shima, 1984). However, a slice through a three-dimensional Voronoi foam cannot itself be the result of a (2-D) Voronoi tessellation. Thus, 3-D work is essential; the first results of our work on this problem are shown here (Fig. 1). The "CfA slices" (De Lapparent et al., 1986; Geller, 1988) do not quite look like the typical 2-D Voronoi shape, but they might resemble a slice through a 3-D foam (Pierre et al., 1988).

2. Kinematics of Voronoi cell formation

When matter streams out of the voids towards the Voronoi skeleton, cell walls form when material from one void encounters that from an adjacent one. If the matter is still gaseous (or collisionless dark matter), only self-gravity will tend to hold it together. However, if galaxies form during the expansion of the voids, they can collect in the walls because of the well-known fact that galaxies have an immense number of internal degrees of freedom, which are excited irreversibly during an encounter (Toomre and Toomre, 1972; Binney and Tremaine, 1987, Chap. 7). Thus, a gas of which the particles are entire galaxies will behave very dissipatively on small length scales.

Accordingly, the kinematics of the formation of Voronoi cells is as follows. Within a void, the mean distance between galaxies increases uniformly in the course of time; this amounts to an excess Hubble expansion about the cell nucleus. When a galaxy tries to enter an adjacent cell, dynamic friction with oncoming galaxies will slow its motion down; on the average, this amounts to the disappearance of its velocity component perpendicular to the cell wall. Thereafter, the galaxy continues to move within the wall, until it tries to enter the next cell; it then loses its velocity component towards that cell, so that the galaxy continues along a filament. Finally, it comes to rest in a node, as soon as it tries to enter a fourth neighbouring void. In a Voronoi foam, there are exactly four cells adjoining each node, and the above process is unique.

An immediate consequence of this kinematic behaviour is, that the density in the walls quickly becomes smaller than in the filaments, which, in turn, remain less dense than the nodes, where all matter eventually congregates. This is the main reason why we identify the nodes with the rich Abell clusters. It is also a reason why the actual mass distribution is expected to look quite sponge-like, rather than a packing of convex cells with an approximately constant density on all surfaces. We believe that, in this respect, our simulations are more realistic than those of Yoshioka and Ikeuchi (1988).

We have constructed three-dimensional Voronoi foams geometrically (Van de Weygaert, 1988) and by means of the above kinematic process (Icke, 1988). A stereogram of a geometrical three-dimensional Voronoi foam with periodic boundary conditions is shown in Fig. 1. A corresponding sequence of kinematic cell formation is shown in Fig. 2. Our aim in these studies is, to obtain the statistical properties of the resulting mass distribution; these are readily compared with the observations, and the Voronoi models can be obtained by extremely modest computational means (the sequence of Fig. 2 took about 20 seconds on a VAX 785.) We emphasize that the Voronoi tessellations are expected to give a correct asymptotic description of *all* structure formation in gravitating pressureless media, except those in which most of the power in the fluctuations occurs on a scale where dissipation is important. Thus, some cold dark matter models fall outside this scope, since their power spectrum has a large amplitude on galactic scales, and galaxies – as we argued above – are very sticky "particles".

The sequence describing the kinematic cell formation was obtained as follows. In a box with dimensions $1 \times 1 \times 1$, assumed

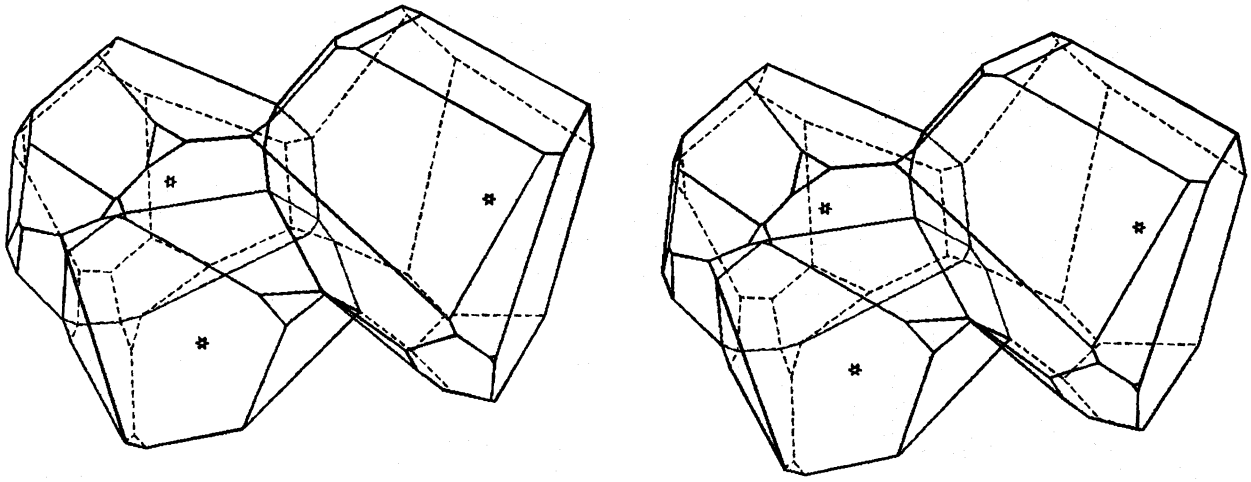

Fig. 1. Stereoscopic pair of three Voronoi cells sharing a common line. The nuclei are indicated by stars. In a stereo viewer, the dashed lines will appear at the rear of the picture. When attempting stereo fusion with crossed eyes, the pictures must be reversed to obtain the correct depth perception. This holds for Fig. 2 too

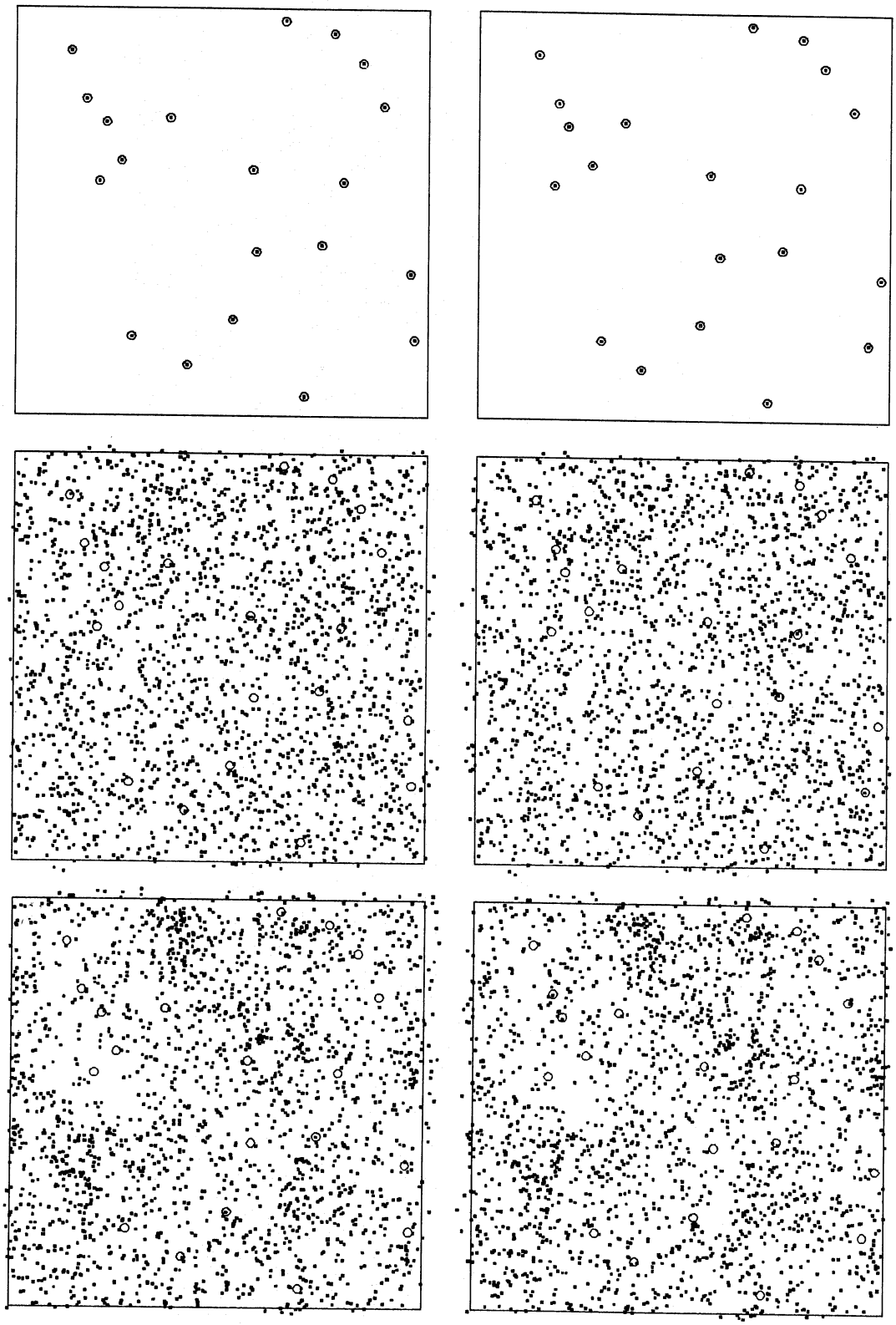

Fig. 2. Time sequence of the formation of kinematic Voronoi cells, as stereo pairs. Counting from top to bottom, one has: first frame, location of the 20 nuclei; these appear as circles in all frames. Second, initial Poissonian distribution of 2000 galaxies. Third, situation at dimensionless time $t = 0.5$; fourth, at $t = 1$; fifth, at $t = 1.5$

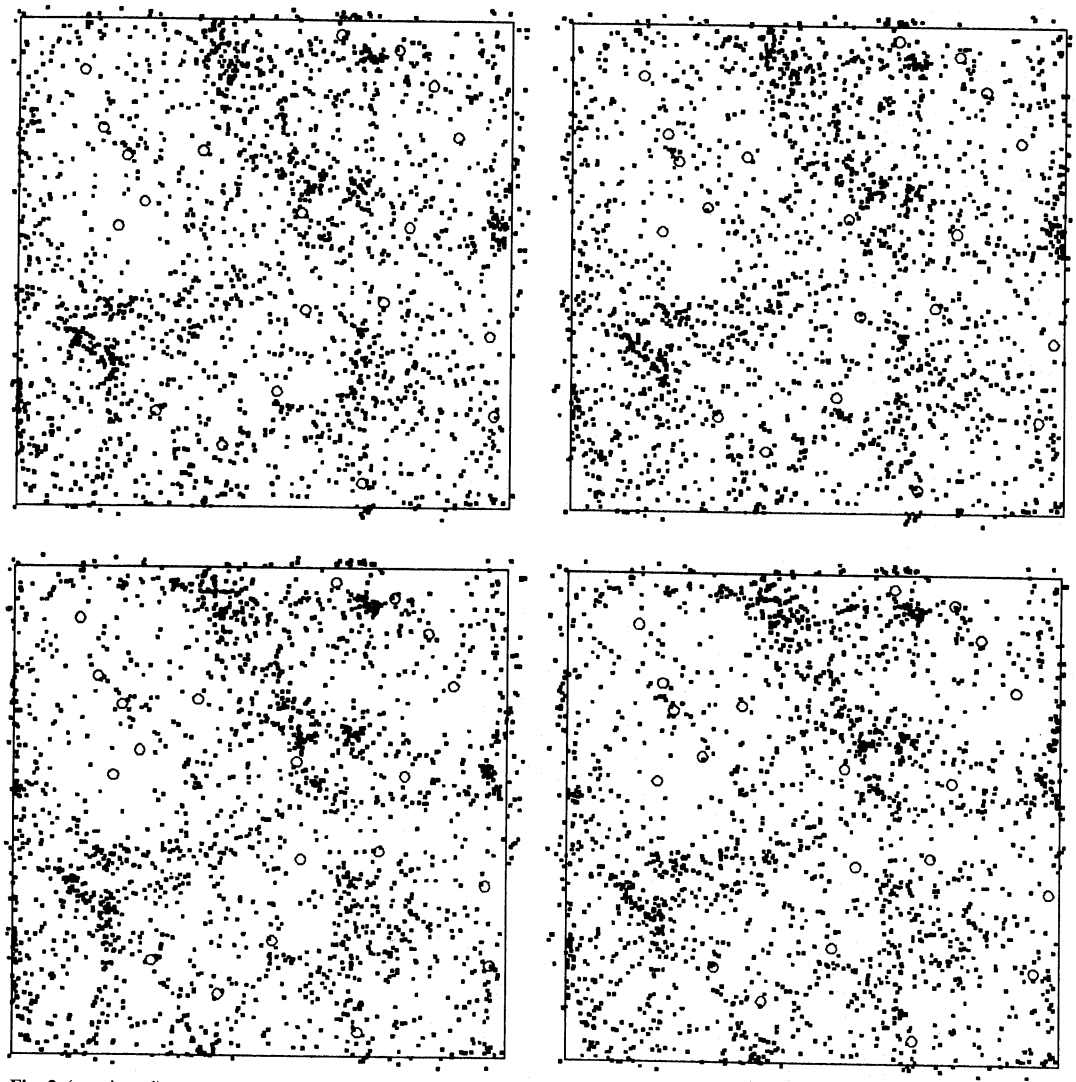

Fig. 2 (continued)

to have periodic boundary conditions, a number N of nuclei was placed at positions $\boldsymbol{e}_n$ by a Poisson process (this defines the length scale of the simulation.) Then a Poissonian distribution of G galaxies at positions $\boldsymbol{x}_g$ was chosen in the same volume. The motion of each galaxy was determined by a sequence of four trajectories.

First, the nearest nucleus was identified (all distance orderings were obtained quickly by means of a *k-d* tree sorting method; Van de Weygaert, 1987). Let its position be called $\boldsymbol{e}_1$. The velocity $\boldsymbol{u}$ of the galaxy at initial position $\boldsymbol{x}_0$ and time $t=0$ was made proportional to the distance to its nucleus, and radially away from it:

$$\boldsymbol{u} = H_* (\boldsymbol{x}_0 - \boldsymbol{e}) . \tag{1}$$

The Voronoi model does not specifically require this functional form, but allows H_* to be a function of $|\boldsymbol{x}_0 - \boldsymbol{e}|$ that smoothly joins H_0 at the void walls. In Eq. (1), the excess Hubble parameter was scaled to $H_* = 1$ (this defines the time scale of the simulation.) The time was increased in steps Δt. Each time step, the new position of the galaxy was obtained from the kinematic prescription

$$\boldsymbol{x}_{\text{new}} = \boldsymbol{x}_{\text{old}} + \Delta t \, \boldsymbol{u} . \tag{2}$$

This step was repeated until the galaxy got closer to another nucleus than the one at the centre of the Voronoi cell from which it departed. At that point, the galaxy would move into an adjacent void, but it is prevented from doing so, and is constrained to move in such a way that its distance to the two nuclei remains the same.

Second, this next-nearest nucleus was identified; call its position $\boldsymbol{e}_2$. The velocity component of $\boldsymbol{u}$ perpendicular to the Voronoi wall (i.e. the component parallel to $\boldsymbol{e}_1 - \boldsymbol{e}_2$) was set to zero according to

$$\boldsymbol{u} \rightarrow \boldsymbol{u} - (\boldsymbol{u} \cdot \boldsymbol{f}_1) \boldsymbol{f}_1 , \tag{3}$$

$$\boldsymbol{f}_1 \equiv \frac{\boldsymbol{e}_1 - \boldsymbol{e}_2}{|\boldsymbol{e}_1 - \boldsymbol{e}_2|} . \tag{4}$$

Notice that this makes $\boldsymbol{u} \cdot (\boldsymbol{e}_1 - \boldsymbol{e}_2) = 0$, while the inner product of $\boldsymbol{u}$ with any vector perpendicular to the line connecting the two nuclei remains unchanged (this connecting line is an edge of a "Delaunay tetrahedron"; see Icke and Van de Weygaert, 1987). On its new track, which lies within a cell wall, the galaxy was advanced according to Eq. (2), until yet a third nucleus came closer than the previous two.

Third, the position e_3 of this nucleus was found, and the unit vectors f_2 and f_3 were determined from

$$f_2 \equiv \frac{e_1 - e_3}{|e_1 - e_3|}, \tag{5}$$

$$f_3 \equiv f_2 \times f_1 . \tag{6}$$

The vector f_2 is parallel to a second Delaunay edge, and f_3 lies along the filament defined by the intersection of the planes that perpendicularly bisect the two Delaunay edges. The component of the galaxy's velocity perpendicular to the filament is now cancelled by putting

$$u \rightarrow (u \cdot f_3) f_3 . \tag{7}$$

The galaxy moves along according to Eq. (2) using this new velocity, thereby keeping the three nuclei at equal distances, until finally a fourth nucleus is approached to within the same distance as the first three. At that point, the galaxy has reached a Voronoi vertex: the point where it is equidistant to four nuclei. In the kinematical model, galaxies stream into such a vertex from all three spatial dimensions, along four joining Voronoi edges (filaments). Thus, the velocity of the galaxy is finally reduced to zero.

Three remarks are in order at this point. First, the encounter of two galaxies converts some of their orbital energy into "heat" (internal motions of the galaxies and stars lost from these systems; Toomre and Toomre, 1972), but unless the galaxies merge, some orbital energy will remain as a general galactic velocity dispersion. Especially in the nodes, this will show up observationally in the form of radial fingers in a position-velocity slice (Giovanelli et al., 1986; De Lapparent et al., 1986). It is relatively easy to incorporate this, by introducing a virial dispersion commensurate with the local galaxy density, but that might be carrying the kinematic approach too far, and detract from its simplicity.

Second, the galactic momentum components perpendicular to walls, in filaments, and in nodes are not exactly cancelled during the encounters we envisage. Rather, these components vanish on the average, because the distances from a wall to its two nearest Voronoi nuclei are equal; the momentum flux (i.e. dynamic pressure) on one side of a wall is equal and opposite to the flux on the other side.

Third, Eq. (2) shows that the spatial dispersion of the galaxies about the exact Voronoi skeleton is given by the mean value of $u\,\Delta t$. This value is on the order of $0.5\,LH_*\,\Delta t$, or about $0.05\,L$ in the simulation shown in Fig. 2, where L is the mean radius of a Voronoi cell. In reality, this dispersion is set by the "stickness" of the interacting galaxies. We have verified that the choice of $L\,\Delta t$ is not important for what follows, provided that $\Delta t \lesssim 0.2$.

3. Angular two-point correlations

In order to compare the Voronoi model with the statistical properties of the observed galaxy distribution, we have determined the two-point correlation functions (Peebles and Hauser, 1974; Peebles, 1974; Peebles, 1980) of the kinematic simulations and of the positions of the Voronoi vertices. First, we consider the kinematic simulations as a model of the distribution of galaxies in the sky. The published observed two-point correlations are angular correlations, which can only be converted to spatial correlations by means of additional algebraic operations. Attempts have been made to obtain spatial galaxy-galaxy correlations, but these results are model dependent because of the need to reconstruct the dimension of depth. Thus, we restrict ourselves here to angular correlations; spatial correlations will be considered in the case of the Voronoi vertices below.

If dA is the area in the sky between distances r and $r+dr$ from a given galaxy, and if dn is the number of galaxies counted in that area, then the two-point correlation function $w(r)$ is defined by

$$dn = \bar{n}\,(1 + w(r))\,dA , \tag{8}$$

where $\bar{n}$ is the average (Poissonian) galaxy density in the sky. The galaxy positions in the $1 \times 1 \times 1$ cube of the kinematic model were projected along the three perpendicular coordinate directions, and the two-point correlations of the resulting three simulated sky maps were calculated. These were then averaged to obtain $w(r)$ (with proper scaling, r corresponds to the customary angular distance θ.) The standard deviations from this average were also obtained. The correlation was performed in linear bins and in logarithmic ones.

The results are shown in Fig. 3. From Eq. (8) it is clear that w cannot be positive everywhere, and indeed the results show that $w = 0$ at $r \approx 0.17$. Now $L \approx 0.18$ in the case of Fig. 3, which was calculated for 20 nuclei, so that we conclude that the two-point correlation dips through zero at about the Voronoi foam scale, climbing back to zero after that. This is entirely as expected: galaxies should be distributed Poissonian on scales larger than those of the voids. The observed amplitude of $w(0)$ is on the order of unity (Peebles, 1974), which in our kinematic models corresponds to a dimensionless time $t \approx 1.8$. An uncertainty is due to the fact that, in reality, the distribution in the sky is not due to a simple projection, but to a projection weighted with the galaxy luminosity function (cf. Limber's equation). We have not attempted to take this into account, because we think that the depth-to-width ratio of observed samples (e.g. Giovanelli et al., 1986, De Lapparent et al., 1986) are close enough to unity to warrant our use of a cube as a representative sample.

When one tries to compare an analytic model like that described above with the observations, there is always the possibility that the match is compromised by various forms of biasing. In order to study a possible effect of this type, we have also calculated the angular correlation function of high-density peaks in the simulations (Icke, 1988). If one only considers galaxies that occupy regions where the local density is one standard deviation above average, the amplitude of w increases by a factor of 1.3; for peaks with amplitude 2σ, the increase is a factor 2.9; and $3\,\sigma$ peaks have an angular correlation amplitude that is 4.9 times higher than that of the unbiased correlation function. In fact, the amplitude w of the angular correlation of galaxies that reside in regions of space where the number density is three standard deviations above average, is about $w(r = 0) = 8$. This comes close to the amplitude for correlations between Abell clusters, as will be seen in the following.

4. Spatial two-point correlations

Next, we consider the spatial correlation of Voronoi nodes. Because we wish to identify these with Abell clusters, this correlation can be compared with observations: the distances to Abell clusters can be estimated accurately enough to allow reasonable estimates of the spatial correlations to be made (Bahcall and Soneira, 1983; Klypin and Kopylov, 1983; Shectman, 1985; Postman et al., 1986; Ling et al., 1987).

The spatial two-point correlation function $\xi(R)$ is defined in the same way as w. Let dV be the volume between the distance R

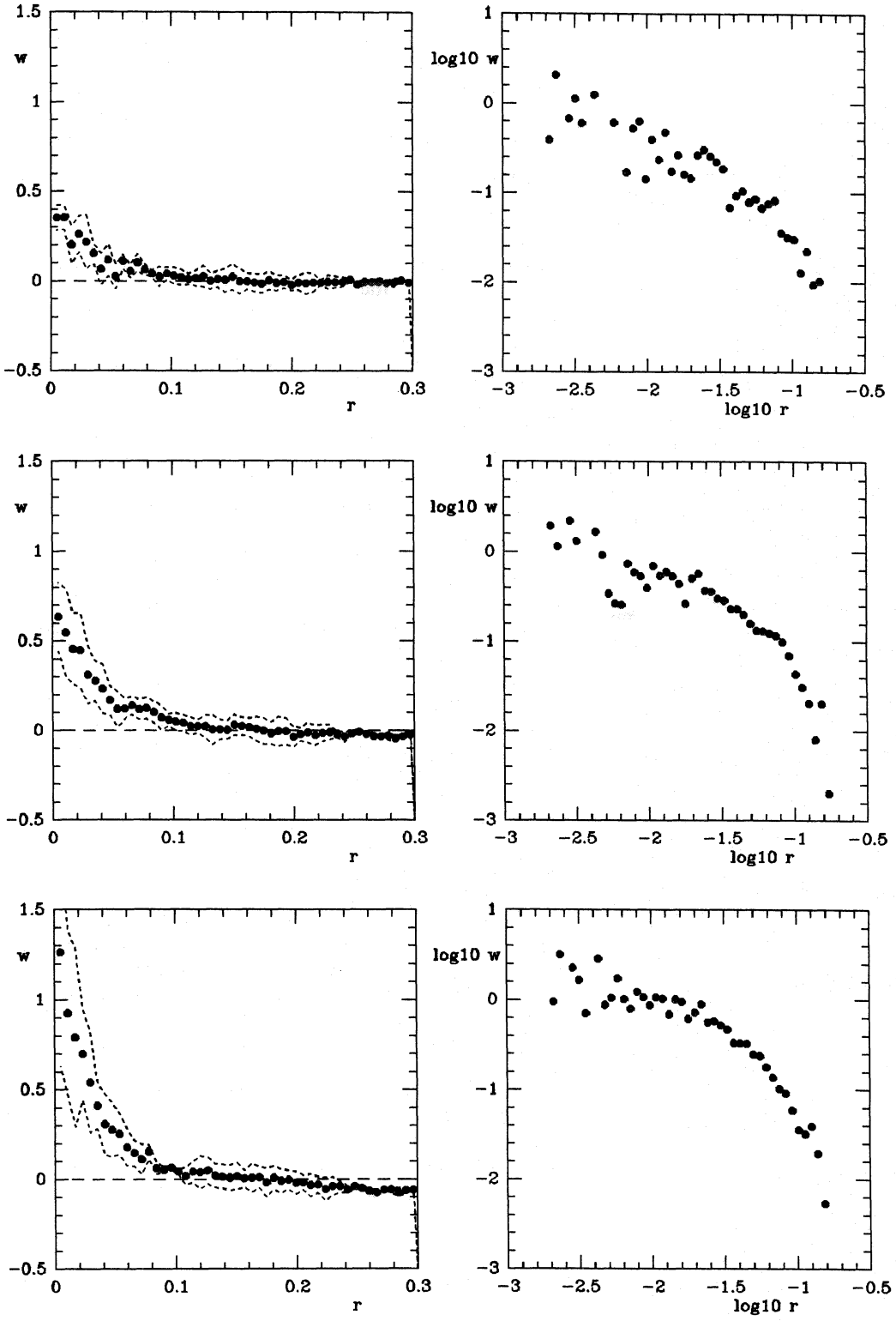

Fig. 3. Angular correlation functions of the galaxy distributions of Fig. 2. Left column, $w(r)$ as determined by counting in linear bins of r. The dashed lines show the $\pm 1\sigma$ deviations as determined from the counting statistics in the three independent coordinate directions. Right column, $\log_{10} w(r)$ as determined by counting in logarithmic bins of r. Top frames, $t = 0.5$; middle, $t = 1$; bottom, $t = 1.5$

and $R+dR$ centered on a given galaxy; if dN is the number of galaxies counted in that volume, then the two-point correlation function is defined by

$$dN = \bar{N}(1+\xi(R))\,dV\,, \tag{9}$$

where $\bar{N}$ is the average (Poissonian) galaxy density in space. A useful way of relating our geometrical Voronoi model to observations is by comparing the spatial correlation function of galaxy clusters, as determined by e.g. Bahcall and Soneira (1983), Shectman (1985), and Postman et al. (1986), with the correlation function of the vertices in the Voronoi tessellation. We identify these vertices as the positions where clusters will form during the formation of the large-scale structure in the Universe (see also e.g. Kofman and Shandarin, 1988), because matter streaming away from four nuclei (cell centres) will collect in these vertices.

Our 3-D Voronoi algorithm (see Van de Weygaert, 1988) was applied to a Poissonian distribution of 1000 nuclei (it takes about 5.5 CPU-minutes on a VAX 785 to constuct a Voronoi foam of 1000 nuclei), giving 6733 vertices ("Abell clusters"). Each computational box had a size of $1\times1\times1$, giving a mean volume of 10^{-3} per cell. The spatial vertex-vertex correlation function ξ_{cc} was determined by using two slightly different estimators. In addition, correlated and anticorrelated distributions of nuclei were considered.

For large sampling radii, ξ_{cc} was determined in the way given by Blanchard and Alimi (1988). This method uses a comparison between two $1\times1\times1$ volumes: one containing the Voronoi vertices, the other containing a Poisson distribution of points (in our case, 25,000). In each volume, a spherical sampling shell $(r-\frac{1}{2}\Delta r,\ r+\frac{1}{2}\Delta r)$ was centered on the coordinates of the i-th Voronoi vertex. Then the number $N^i_{dd}(r)$ is the total number of vertices in the Voronoi sample encompassed by the shell; $N^i_{dp}(r)$ is the total number of points in the same interval in the Poisson distribution. Summed over i, one obtains $N_{dd}(r)$ and $N_{dp}(r)$. Then the correlation function is

$$\xi_{cc}(r) = \frac{N_{dd}(r)}{N_{dp}(r)}\frac{n_p}{\bar{n}} - 1\,, \tag{10}$$

in which $\bar{n}$ is the density of clusters (Voronoi vertices) and n_p is the density of Poisson points. In this way, one can neatly correct for edge effects without losing too much information.

Because $N_{dp}(r)$ becomes very small at small radii (the number of Poisson points is proportional to r^2), the $\sqrt{N}$ fluctuations in N_{dp} get too large, causing huge errors in the estimated ξ. Therefore, another estimator was used when $\sqrt{N}$ fluctuations exceeded 10%:

$$\xi_{cc}(r) = \frac{N_{dd}(r)}{\bar{n}\sum_{i=1}^{M}\delta V_i} - 1\,, \tag{11}$$

where $N_{dd}(r)$ is the total number of pairs in the Voronoi vertex catalog determined by counting around each vertex i the number of vertices in a shell $(r-\frac{1}{2}\Delta r,\ r+\frac{1}{2}\Delta r)$ if the vertex i had at least a distance $r+\frac{1}{2}\Delta r$ from the edge of the catalog volume; N_{dd} is the total number of all these pairs. Consequently, a pair (i,j) will be counted twice if both vertices i and j lie further than a distance $r+\frac{1}{2}\Delta r$ from the walls of the catalog cube. The number $\sum_{i=1}^{M}\delta V_i$ is the sum of the shell volumes around the M vertices included in the count.

Because the use of estimator (11) was limited to a radius of 0.5% of the size of the box (i.e. 0.005), in the case of a uniform distribution of points only 3% of the pairs is excluded from N_{dd}, which won't increase the fluctuations in the counts significantly. On small scales, the vertices do not form a uniform distribution, as will be seen below, but they do so on larger scales.

The resulting cluster-cluster correlation function in our Voronoi model is shown in Fig. 4, for a uniform distribution of nuclei. The function can be approximated very well by a power law, in this case with a slope of 1.97. In the case of moderately correlated expansion centres, the slope turned out to be 1.88. Both numbers look quite nice compared with the observationally determined slope of $\gamma = 1.8\pm0.3$ (cf. Weinberg et al., 1988).

The amplitude of our correlation function is $r_0 = 3.00\ 10^{-2}$; a break appears around $\xi \approx 0.5$, caused by the zero crossing of ξ near $r_a \approx 5.2\ 10^{-2}$. If we normalize the amplitude of ξ_{cc} to the mean distance $\bar{n}^{-1/3}$ between clusters, (with $\bar{n}$ being the mean number density of clusters), we get an estimate for our r_0. Blumenthal et al. (1988) give 55 Mpc for the Abell clusters of richness 1 and above. This corresponds to $6733^{-1/3} \approx 5.2\ 10^{-2}$ in the Voronoi vertex sample; thus, $r_0 \approx 32$ Mpc, which is the upper limit given in the estimate of r_0 in the review by Bahcall (1988). In Fig. 4 we have also plotted the function $1+\xi$ as calculated from the same Voronoi foam. As in the case of ξ, one can approximate $1+\xi$ by a power law. The best fit to our results is

$$1+\xi(r) = (3.94\ 10^{-2}/r)^{1.77}\,, \tag{12}$$

which has a slope that is statistically indistinguishable from the observed value 1.8. Furthermore, when normalizing in the same way as above, we find that $\xi(r_0) = 1$ gives $r_0 = 27$ Mpc.

The observationally determined cluster-cluster correlation function and our vertex-vertex correlation differ in the position of the break, which occurs around 54 Mpc according to our Voronoi model, while in the real world the power law extends to 80–90 Mpc (Postman et al., 1986). A possible solution to this problem is that the nuclei are correlated. We have begun to investigate this effect; the first results show that the power law is in fact extended to larger scales. Another possibility is, that the Voronoi model and the Abell classification do not attach equal weights to vertices and to clusters. In the Voronoi model, each vertex is treated equally with the others, whereas in the Abell catalog only outstanding mass concentrations are counted. This difference is possibly important, because Voronoi vertices that are close together effectively attract less mass than widely spaced vertices. This biases our model towards the smaller length scales, when compared with the observations.

Geometrically, our model bears some resemblance to that of Weinberg et al. (1988), who found that clusters formed by a confluence of triples of bubbles (expanding due to primordial explosions) show a power law two-point correlation too.

5. Concluding remarks

Like any model, the Voronoi tessellation is only an approximation of reality. In the case of our simulations of the formation of the Voronoi voids, we are limited by the fact that only the kinematic behaviour is included. We are in the process of improving on this, by making dynamical calculations of the formation of walls, filaments, and nodes. In the case of the spatial two-point correlations, our results are approximate in the sense that the mathematical Voronoi skeleton is only asymptotic, indicating the locus where matter will congregate in the limit for large times. But the accumulation of matter is fastest in the nodes; therefore, we are

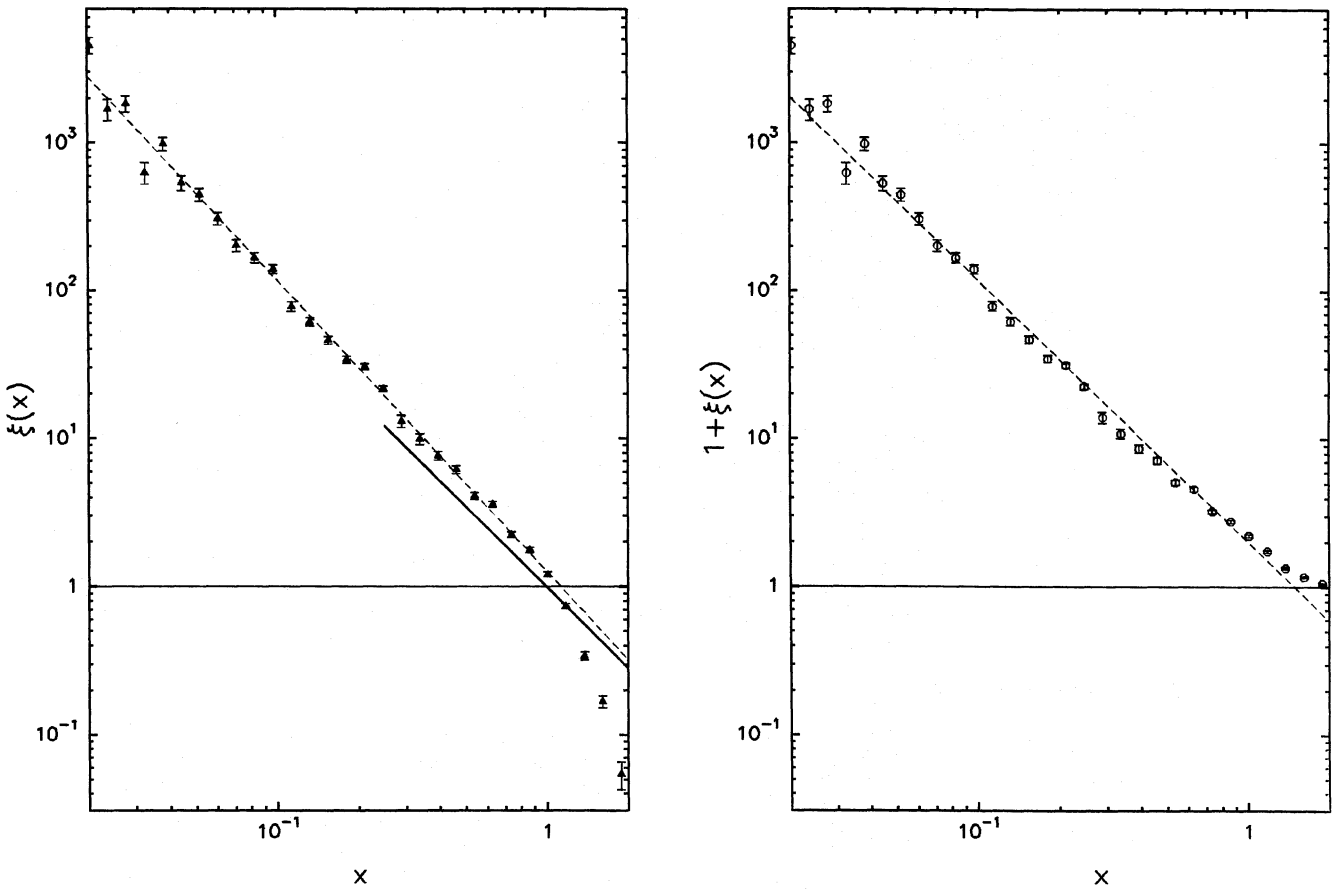

Fig. 4. Spatial vertex-vertex correlation functions of a Voronoi foam with 1000 Poissonian nuclei. The left panel shows ξ, on the right is $1+\xi$. Both have been plotted as functions of the dimensionless quantity $x \equiv 2r/\bar{d}$, in which $\bar{d}$ is the mean separation between vertices. The error bars were determined on the basis of $\sqrt{N}$ errors in the estimators. The dashed lines are least-squares fits to all data points except the last three. One finds $\xi(x) = (1.13/x)^{1.97}$ and $1+\xi(x) = (1.94/x)^{1.77}$. The heavy solid line is an approximate fit to the observational data

quite confident that the correlation behaviour of these points is a rather robust property of the model.

Although the resulting estimate of our cluster-cluster correlation function is not ideal, we think that it is very remarkable that such a simple geometrical picture can give an estimate of ξ_{cc} nearly in accordance with observations. Details might slightly change the quantitative conclusions; for example, in the case of correlated nuclei the slope of the correlation function becomes somewhat shallower, while the position of the break shifts to a larger scale, although the effect is surprisingly weak. Clustered nuclei may be more realistic, because the expansion centres are the positions of the large negative density peaks in a gaussian random field, producing the voids in the Universe, of which Bardeen et al. (1986) showed that they were correlated.

Notwithstanding such details, we expect that our conclusions will remain essentially the same. It looks as if the cluster-cluster correlation function on both small and large scales is determined by the cell structure in the Universe (De Lapparent et al., 1986), which might explain the remarkable fact that both for $\xi \gg 1$ and for $\xi < 1$ the slope of $\xi(r)$ is the same. Moreover, numerical simulations (Centrella and Melott, 1983; Davis et al., 1985) indicate that, during the evolution of the structure in the Universe, the slope of the galaxy-galaxy correlation function ξ_{gg} gets steeper with time, having reached a value of 1.8 by now, due to the effects of gravitation. This might be nothing but a reflection of the fact that galaxies tend to congregate more and more towards rich clusters, first going from a nearly uniform distribution to clustering in pancakes, then going to filaments, and finally to vertices, leaving a Universe with nothing more than huge clusters. In the end, this sequence of events produces a ξ_{gg} with a slope around 2, dictated by the positions of the clusters in the vertices of the cell texture of the Universe.

Acknowledgements. We are indebted to Bernard Jones for stimulating discussions and for his hospitality towards R.v.d.W. at NORDITA, to Peter Katgert for a critical reading of the manuscript to J.H. Oort for his continuing interest in this project, and to the referee (A.L. Melott) for a swift and pertinent appraisal of an earlier version of this article. Partial travel funds for R.v.d.W. were provided by the Leids Kerkhoven-Bosscha Fonds.

References

Bahcall, N.A.: 1988, *Ann. Rev. Astron. Astrophys.* **26**, (in press)
Bahcall, N.A., Soneira, R.M.: 1983, *Astrophys. J.* **270**, 20
Bardeen, J., Bond, J.R., Kaiser, N., Szalay, A.: 1986, *Astrophys. J.* **304**, 15
Binney, J., Tremaine, S.: 1987, *Galactic Dynamics*, Princeton University Press

Blanchard, A., Alimi, J.-M.: 1988, preprint
Blumenthal, G.R., Dekel, A., Primack, J.R.: 1988, *Astrophys. J.* **326**, 539
Centrella, J., Melott, A.: 1983, *Nature* **305**, 196
Davis, M., Efstathiou, G., Frenk, C.S., White, S.D.M.: 1985, *Astrophys. J.* **292**, 371
De Lapparent, V., Geller, M., Huchra, J.: 1986, *Astrophys. J. Letters* **302**, L 1
Einasto, J., Joêveer, M., Saar, E.: 1980, *Monthly Notices Roy. Astron. Soc.* **193**, 353
Giovanelli, R., Haynes, M.P., Chincarini, G.L.: 1986, *Astrophys. J.* **300**, 77
Geller, M.: 1988, in *Large scale structures in the Universe*, 17th Saas-Fee Course, eds. L. Martinet, M. Mayor, Geneva Observatory, p. 69
Gott, J.R., Melott, A.L., Dickinson, M.: 1986, *Astrophys. J.* **306**, 341
Icke, V.: 1972, Ph. D. Thesis, Leiden
Icke, V.: 1973, *Astron. Astrophys.* **27**, 1
Icke, V.: 1984, *Monthly Notices Roy. Astron. Soc.* **206**, 1 P
Icke, V.: 1988 (in preparation)
Icke, V., Van de Weygaert, R.: 1987, *Astron. Astrophys.* **184**, 16
Ikeuchi, S.: 1981, *Publ. Astron. Soc. Japan* **33**, 211
Klypin, A.A., Kopylov, A.I.: 1983, *Soviet Astron. Letters* **9**, 41
Kirshner, R.P., Oemler, A., Schechter, P.L., Shectman, S.A.: 1981, *Astrophys. J. Letters* **248**, L 57
Kirshner, R.P., Oemler, A., Schechter, P.L., Shectman, S.A.: 1987, *Astrophys. J.* **314**, 493
Kofman, A.L., Shandarin, S.F.: 1988, *Nature* **334**, 129
Lin, C.C., Mestel, L., Shu, F.H.: 1965, *Astrophys. J.* **142**, 1431
Ling, E.N., Frenk, C.S., Barrow, J.D.: 1986, *Monthly Notices Roy. Astron. Soc.* **223**, 21 P
Lynden-Bell, D.: 1964, *Astrophys. J.* **139**, 1195
Matsuda, T., Shima, E.: 1984, *Prog. Theor. Phys.* **71**, 855
Melott, A.L.: 1983, *Monthly Notices Roy. Astron. Soc.* **205**, 637
Melott, A.L., Weinberg, D.H., Gott, J.R.: 1988, *Astrophys. J.* **328**, 50
Oort, J.H.: 1983, *Ann. Rev. Astron. Astrophys.* **21**, 373
Ostriker, J.P., Cowie, L.: 1981, *Astrophys. J. Letters* **243**, L 127
Peebles, P.J.E.: 1974, *Astrophys. J. Suppl.* **28**, 37
Peebles, P.J.E.: 1980, *The Large Scale Structure of the Universe*, Princeton University Press
Peebles, P.J.E., Hauser, M.G.: 1974, *Astrophys. J. Suppl.* **28**, 19
Pierre, M., Shaver, P.A., Iovino, A.: 1988, *Astron. Astrophys.* **179**, L 3
Postman, M., Geller, M.J., Huchra, J.P.: 1986, *Astron. J.* **91**, 1267
Shectman, S.A.: 1985, *Astrophys. J. Suppl.* **57**, 77
Toomre, A., Toomre, J.: 1972, *Astrophys. J.* **178**, 623
Van de Weygaert, R.: 1987, B.Sc. Thesis, Leiden
Van de Weygaert, R.: 1988, in preparation
Voronoi, G.: 1908, *J. reine angew. Math.* **134**, 198
Weinberg, D.H., Gott, J.R., Melott, A.L.: 1987, *Astrophys. J.* **321**, 2
Weinberg, D.H., Ostriker, J.P., Dekel, A.: 1988, preprint
Yoshioka, S., Ikeuchi, S.: 1988, preprint
Zel'dovich, Y.B.: 1970, *Astron. Astrophys.* **5**, 84